Title: Structural basis for selective stalling of human ribosome nascent chain complexes by a drug-like molecule

Authors: Wenfei Li[1,2], Kim F. McClure[4], Elizabeth Montabana[2], Spiros Liras[4], Robert Dullea[5] and Jamie H. D. Cate[1,2,3]*

Affiliations:

[1]Department of Molecular & Cell Biology, University of California, Berkeley, California 94720, USA.

[2]Molecular Biophysics and Bioimaging Division, Lawrence Berkeley National Laboratory, Berkeley, California 94720, USA.

[3]Department of Chemistry, University of California, Berkeley, California 94720, USA.

[4]Pfizer Medicinal Chemistry, Pfizer Worldwide Research and Development, Cambridge, Massachusetts 02139, United States of America

[5]Cardiovascular, Metabolic and Endocrine Disease Research Unit, Pfizer Worldwide Research and Development, Cambridge, Massachusetts 02139, United States of America,

*Correspondence to: jcate@lbl.gov.

Abstract: Small molecules that target the ribosome generally have a global impact on protein synthesis. However, the drug-like molecule PF-06446846 (PF846) binds the human ribosome and selectively blocks the translation of a small subset of proteins by an unknown mechanism. In high-resolution cryo-electron microscopy (cryo-EM) structures of human ribosome nascent chain complexes stalled by PF846, PF846 binds in the ribosome exit tunnel in a eukaryotic-specific pocket formed by the 28S ribosomal RNA (rRNA), and redirects the path of the nascent polypeptide chain. PF846 arrests the translating ribosome in the rotated state, with peptidyl-tRNA occupying a mixture of A/A and hybrid A/P sites. These results provide a structural foundation for a new strategy for developing small molecules that selectively inhibit the production of proteins of therapeutic interest.

One sentence summary: A drug-like small molecule binds in a newly-identified site in the exit tunnel of the human ribosome and selectively stalls translation by trapping the rotated state of the ribosome, likely preventing efficient translocation of the mRNA and tRNAs.

Main Text:

Most compounds that target the ribosome affect a large number of mRNAs through general inhibition of translation initiation or elongation (*1-3*). Furthermore, these compounds almost exclusively act as broad-spectrum inhibitors, displaying little sequence specificity (*4*). Many studies have revealed how these compounds bind the translating ribosome and inhibit its function (*5-9*). Recently, we described the small molecule PF846 that selectively blocks translation of individual mRNAs by human ribosomes (*10, 11*). However, a mechanism to account for the ability of PF846 to selectively inhibit human protein synthesis remains unknown.

PF846 blocks production of proprotein convertase subtilisin/kexin type 9 (PCSK9)–an important target for regulating plasma low-density lipoprotein cholesterol levels–by interfering with the elongation phase of translation (*11-13*). PF846 selectively stalls the ribosome on very few translated protein nascent chains, generally early in their formation and with no definitive sequence pattern (*11*). To gain insight into the mode of action of PF846 in targeting the human ribosome and specific nascent chains, and to identify principles for future drug development, we determined structures of PF846 stalled ribosome nascent chain (RNC) complexes using single-particle cryo-EM. Since the stalling sequences in most proteins affected by PF846 occur near the N-terminus and would therefore reside in the ribosome exit tunnel (*11*), we first identified conditions for affinity purification of stable PF846-stalled RNCs from *in vitro* translation reactions in human cell extracts. The calcium-dependent cell-cell adhesion glycoprotein Cadherin-1 (CDH1) (*11, 14*) is stalled near its C-terminus by PF846, enabling the extension of the peptide N-terminus beyond the confines of the ribosomal exit tunnel.

Appending an N-terminal affinity tag followed by the CDH1 cadherin-V domain and the nascent chain sequences targeted by PF846 did not disrupt the ability of PF846 to stall translation and allowed formation and purification of stable PF846-stalled RNCs (**Fig. 1A, 1B**, **fig. S1**).

To investigate how PF846 stalls specific nascent chain sequences in the human ribosome, we used cryo-EM to determine structures of PF846-stalled CDH1 or PCSK9 ribosome nascent chain complexes (CDH1-RNC or PCSK9-RNC, respectively) (**fig. S2, fig. S3, table S1**). In both CDH1-RNC and PCSK9-RNC samples, particle sorting of the purified RNCs revealed two populations of ribosomes in the rotated state: one with A/A site peptidyl-tRNA (i.e. nascent chain-tRNA, or NC-tRNA), and the other with hybrid A/P site NC-tRNA. Both also included tRNA in the hybrid P/E site and PF846 bound in the ribosome exit tunnel (**Fig. 1C, fig. S4A** and **S4B**). The following analyses describe the CDH1-RNCs due to the higher-quality CDH1-RNC cryo-EM maps, although we observe similar behavior for the PCSK9-RNCs, as shown in the supplementary figures.

The CDH1-RNC complexes with hybrid A/P site NC-tRNA or with A/A site NC-tRNA yielded cryo-EM maps with an average resolution of 3.7 Å and 4.3 Å, respectively (**Fig. 1C, 1D and fig. S2**). The hybrid A/P NC-tRNA represents a mixture of tRNAs, as inferred from the EM map density for nucleotide bases in the codon-anticodon base pairs (**fig. S5** and **fig. S6**), consistent with the clustering of stall sites spanning multiple codons observed by ribosome profiling (*11*). We also observed a small population of stalled RNCs in the non-rotated state bearing a P/P-site NC-tRNA and PF846 in our samples (**fig. S2, fig. S3 and fig. S4C**). Interestingly, this population appeared in higher abundance when the RNC sample was purified using a short isolation time prior to

making cryo-EM grids (**fig. S3B**). These results suggest that the non-rotated RNC is a transient state during PF846 mediated translation stalling. Collectively, our findings suggest that PF846 preferentially stalls RNCs in the rotated state, while the non-rotated state with P/P-site NC-tRNA can be resolved during translation in the presence of PF846.

In the rotated-state RNCs with A/P NC-tRNAs, PF846 occupies a binding pocket in a groove of the ribosomal exit tunnel formed by universally conserved 28S rRNA nucleotides (*15*) and a stretch of the stalled nascent chain (**Fig. 2**). PF846 was fit to the density by evaluating its X-ray structures (*11*) and low energy conformations based on quantum mechanical assessment of accessible torsion angles (**fig. S7, table S2**). Consistent with PF846 binding to non-translating 80S ribosomes (*11*), contacts with 28S rRNA make up the bulk of the small molecule interactions with the ribosome (**Fig. 2**, **fig. S7**). The piperidine ring extends into the rRNA binding pocket, contacting nucleotides C1576, G1577, G1579, A1583 and U1584 (**Fig. 2E**). The chloro-pyridine and amide linkage also form hydrogen bonds with highly conserved nucleotides G1577 and G1579 (**Fig. 2F** and **2G**). Additionally, the interaction is stabilized by U4517, which forms a stacking interaction with the chloro-pyridine ring (**Fig. 2H**). To explore the structural basis for PF846 action on eukaryotic but not bacterial ribosomes (*11*), we aligned the small molecule-binding pocket with the corresponding region in the *E. coli* ribosome (**Fig. 2A, 2B** and **fig. S8**). Phylogenetic analysis revealed key changes to the nucleotide pattern in 23S rRNA in the large ribosomal subunit of bacteria (*15*) (**Fig. 2A** and **2B**). Whereas nucleotides C1576, G1577 and G1579 in the human ribosome are highly complementary to the conformation of PF846 (**Fig. 2F** and **2G**), nucleotides *N1*-methyl-

G745 and ψ746 in bacterial 23S rRNA would clash with the compound (**fig. S8C** and **S8D**). Furthermore, whereas U4517 in the human ribosome stacks on the chloropyridine ring in PF846 (**Fig. 2H**), the corresponding nucleotide in bacterial 23S rRNA (U2609) would sterically clash with PF846 (**fig. S8E**). Taken together, these distinctions in nucleotide identity and positions help explain PF846's specificity for eukaryotic ribosomes.

The triazolopyridine ring system of PF846 faces the ribosome tunnel and is the only part of the molecule with direct interaction with the stalled nascent chain (**Fig. 3**, **fig. S9** and **S10**). Notably, the triazolopyridine moiety has incomplete density that may be caused by the flexibility of this region during nascent chain elongation (**fig. S7**). Interestingly, the density for the nascent chains in the RNCs with A/P NC-tRNA was mostly well defined in the ribosome exit tunnel with a local resolution of ~4 Å, although they are likely comprised of different sequences superimposed on each other corresponding to the cluster of stalled states spanning multiple mRNA codons (**fig. S5** and **S6**) (*11*). Both the CDH1 and PCSK9 nascent chains have similar geometry and adopt a predominantly extended conformation in the exit tunnel (*16*) (**fig. S9** and **S10**). The nascent chain spans ~9 residues between the C-terminus of the nascent chains bonded to the 3'-CCA end of A/P site tRNA in the peptidyl transferase center (PTC) and the small molecule binding site (**Fig. 3A** and **fig. S10**). These residues engage in multiple interactions with nucleotides in 28S rRNA of the 60S subunit, including U4493, U4414, and A3879 (**Fig. 3A** and **fig. S10**). Past the compound-binding pocket (i.e. in the N-terminal direction), the nascent chain is stabilized by ribosomal proteins uL4 and uL22, along with A1582 and C2773 in 28S rRNA (**Fig. 3A** and **fig. S10**). Most reported

RNC structures have “kinks” in the ribosome exit tunnel proximal to the PTC (*17*). The CDH1 and PCSK9 nascent chains also have a kink in their structures between the PTC active site and PF846-binding pocket (**Fig. 3A, figS9** and **fig. S10**), but these adopt a different geometry when compared to stalled human cytomegalovirus (hCMV) and signal recognition particle (SRP) nascent chains (*18, 19*) (**Fig. 3B** and **3C**). In the CDH1-RNC and PCSK9-RNC structures, the “kinks” assume more acute angles, to make enough space for the bound small molecule (**Fig. 3A, fig. S9** and **S10**), whereas the hCMV and SRP NC positions would occlude PF846 binding (**Fig. 3B** and **3C**).

PF846 stalls translation of the ribosome predominantly in the rotated state, yet somehow blocks the action of eEF2, the GTPase which promotes mRNA and tRNA translocation to the next codon position (*20*). In bacterial translation, which is better understood (*21, 22*), translocation proceeds through a series of ribosome rotated states, in which the peptidyl-tRNA body and 3’-CCA end move independently from one another, transiting from an A/A site with 3’-CCA end base pairing with the large subunit rRNA A-loop, to an A/A site with 3’-CCA end base pairing with the large subunit rRNA P-loop, and finally to an A/P site with 3’-CCA base pairing with the P-loop (*23*). At this point, EF-G (the bacterial homologue of eEF2) can catalyze the remaining conformational changes required for complete translocation of the mRNA and tRNAs (*21, 22*). In the PF846-stalled complexes, we observe populations with A/A and A/P NC-tRNAs. However, the A/P-tRNA exhibits flexible base pairing of the 3’-CCA end with the ribosomal P-loop (**Fig. 4, fig. S11**). We propose that PF846 inhibits rapid translocation of specific nascent chains by preventing the peptidyl-tRNA from binding stably in the

hybrid A/P site, which requires the tRNA 3'-CCA end to properly base pair with 28S rRNA nucleotides in the P-loop.

The present structures of PF846-stalled CDH1 and PCSK9-RNCs provide the first molecular detail for the selective stalling of nascent chains in human ribosomes by a small molecule. PF846 binds a newly-identified small molecule-binding pocket in the exit tunnel of the human ribosome and traps select RNCs predominantly in the rotated state (**Fig. 4C**). However, redirection of the nascent chain by PF846 seems to prevent stable base pairing of the NC-tRNA 3'-CCA end with the ribosomal P-loop, likely making these RNCs poor substrates for the GTPase eEF2 responsible for mRNA and tRNA translocation. Stalling of RNCs in the rotated state may be a critical determinant of PF846 selectivity by also evading cellular quality control pathways that recognize aberrantly stalled ribosomes and initiate recycling (*24-28*). For example, Pelota (PELO, Dom34 in yeast) and its cofactors are involved in ribosome-associated quality control pathways that recognize stalled ribosome with an empty A site, to which Pelota binds and promotes ribosome subunit dissociation (*29-33*). Consistent with the hypothesis that quality control pathways resolve PF846-stalled RNCs, ribosome profiling experiments did not reveal a buildup of stalled RNCs in cells treated with PF846 (*11*). The experimental methods presented here provide a means for probing the sequence specificity of PF846-like compounds, and should enable the discovery of other compounds that target the translating human ribosome for therapeutic effect.

References:

1. J. Lin, D. Zhou, T. A. Steitz, Y. S. Polikanov, M. G. Gagnon, Ribosome-Targeting Antibiotics: Modes of Action, Mechanisms of Resistance, and Implications for Drug Design. *Annu Rev Biochem*, (2018) [Epub ahead of print].

2. K. L. Rinehart, Jr., J. B. Gloer, R. G. Hughes, Jr., H. E. Renis, J. P. McGovren, E. B. Swynenberg, D. A. Stringfellow, S. L. Kuentzel, L. H. Li, Didemnins: antiviral and antitumor depsipeptides from a caribbean tunicate. *Science* **212**, 933-935 (1981).

3. A. G. Myasnikov, S. Kundhavai Natchiar, M. Nebout, I. Hazemann, V. Imbert, H. Khatter, J. F. Peyron, B. P. Klaholz, Structure-function insights reveal the human ribosome as a cancer target for antibiotics. *Nat Commun* **7**, 12856 (2016).

4. M. M. Almutairi, M. S. Svetlov, D. A. Hansen, N. F. Khabibullina, D. Klepacki, H. Y. Kang, D. H. Sherman, N. Vazquez-Laslop, Y. S. Polikanov, A. S. Mankin, Co-produced natural ketolides methymycin and pikromycin inhibit bacterial growth by preventing synthesis of a limited number of proteins. *Nucleic Acids Res* **45**, 9573-9582 (2017).

5. K. Kannan, A. S. Mankin, Macrolide antibiotics in the ribosome exit tunnel: species-specific binding and action. *Ann N Y Acad Sci* **1241**, 33-47 (2011).

6. D. N. Wilson, Ribosome-targeting antibiotics and mechanisms of bacterial resistance. *Nat Rev Microbiol* **12**, 35-48 (2014).

7. N. Garreau de Loubresse, I. Prokhorova, W. Holtkamp, M. V. Rodnina, G. Yusupova, M. Yusupov, Structural basis for the inhibition of the eukaryotic ribosome. *Nature* **513**, 517-522 (2014).

8. J. Marks, K. Kannan, E. J. Roncase, D. Klepacki, A. Kefi, C. Orelle, N. Vazquez-Laslop, A. S. Mankin, Context-specific inhibition of translation by ribosomal antibiotics targeting the peptidyl transferase center. *Proc Natl Acad Sci U S A* **113**, 12150-12155 (2016).

9. S. C. Blanchard, B. S. Cooperman, D. N. Wilson, Probing translation with small-molecule inhibitors. *Chem Biol* **17**, 633-645 (2010).

10. N. Sonenberg, A. G. Hinnebusch, Regulation of translation initiation in eukaryotes: mechanisms and biological targets. *Cell* **136**, 731-745 (2009).

11. N. G. Lintner, K. F. McClure, D. Petersen, A. T. Londregan, D. W. Piotrowski, L. Wei, J. Xiao, M. Bolt, P. M. Loria, B. Maguire, K. F. Geoghegan, A. Huang, T. Rolph, S. Liras, J. A. Doudna, R. G. Dullea, J. H. Cate, Selective stalling of human translation through small-molecule engagement of the ribosome nascent chain. *PLoS Biol* **15**, e2001882 (2017).

12. D. N. Petersen, J. Hawkins, W. Ruangsiriluk, K. A. Stevens, B. A. Maguire, T. N. O'Connell, B. N. Rocke, M. Boehm, R. B. Ruggeri, T. Rolph, D. Hepworth, P. M. Loria, P. A. Carpino, A Small-Molecule Anti-secretagogue of PCSK9 Targets the 80S Ribosome to Inhibit PCSK9 Protein Translation. *Cell Chem Biol* **23**, 1362-1371 (2016).

13. D. Urban, J. Poss, M. Bohm, U. Laufs, Targeting the proprotein convertase subtilisin/kexin type 9 for the treatment of dyslipidemia and atherosclerosis. *J Am Coll Cardiol* **62**, 1401-1408 (2013).

14. S. Hirano, A. Nose, K. Hatta, A. Kawakami, M. Takeichi, Calcium-dependent cell-cell adhesion molecules (cadherins): subclass specificities and possible involvement of actin bundles. *J Cell Biol* **105**, 2501-2510 (1987).

15. J. J. Cannone, S. Subramanian, M. N. Schnare, J. R. Collett, L. M. D'Souza, Y. Du, B. Feng, N. Lin, L. V. Madabusi, K. M. Muller, N. Pande, Z. Shang, N. Yu, R. R. Gutell, The comparative RNA web (CRW) site: an online database of comparative sequence and structure information for ribosomal, intron, and other RNAs. *BMC Bioinformatics* **3**, 2 (2002).

16. D. N. Wilson, R. Beckmann, The ribosomal tunnel as a functional environment for nascent polypeptide folding and translational stalling. *Curr Opin Struct Biol* **21**, 274-282 (2011).

17. T. Su, J. Cheng, D. Sohmen, R. Hedman, O. Berninghausen, G. von Heijne, D. N. Wilson, R. Beckmann, The force-sensing peptide VemP employs extreme compaction and secondary structure formation to induce ribosomal stalling. *Elife* **6**, e25642 (2017).

18. S. Matheisl, O. Berninghausen, T. Becker, R. Beckmann, Structure of a human translation termination complex. *Nucleic Acids Res* **43**, 8615-8626 (2015).

19. R. M. Voorhees, R. S. Hegde, Structures of the scanning and engaged states of the mammalian SRP-ribosome complex. *Elife* **4**, e07975 (2015).

20. T. E. Dever, R. Green, The elongation, termination, and recycling phases of translation in eukaryotes. *Cold Spring Harb Perspect Biol* **4**, a013706 (2012).

21. M. R. Wasserman, J. L. Alejo, R. B. Altman, S. C. Blanchard, Multiperspective smFRET reveals rate-determining late intermediates of ribosomal translocation. *Nat Struct Mol Biol* **23**, 333-341 (2016).

22. R. Belardinelli, H. Sharma, N. Caliskan, C. E. Cunha, F. Peske, W. Wintermeyer, M. V. Rodnina, Choreography of molecular movements during ribosome progression along mRNA. *Nat Struct Mol Biol* **23**, 342-348 (2016).

23. L. Wang, R. B. Altman, S. C. Blanchard, Insights into the molecular determinants of EF-G catalyzed translocation. *RNA* **17**, 2189-2200 (2011).

24. A. van Hoof, E. J. Wagner, A brief survey of mRNA surveillance. *Trends Biochem Sci* **36**, 585-592 (2011).

25. F. J. LaRiviere, S. E. Cole, D. J. Ferullo, M. J. Moore, A late-acting quality control process for mature eukaryotic rRNAs. *Mol Cell* **24**, 619-626 (2006).

26. C. A. P. Joazeiro, Ribosomal Stalling During Translation: Providing Substrates for Ribosome-Associated Protein Quality Control. *Annu Rev Cell Dev Biol* **33**, 343-368 (2017).

27. O. Brandman, R. S. Hegde, Ribosome-associated protein quality control. *Nat Struct Mol Biol* **23**, 7-15 (2016).

28. M. H. Bengtson, C. A. Joazeiro, Role of a ribosome-associated E3 ubiquitin ligase in protein quality control. *Nature* **467**, 470-473 (2010).

29. K. Ikeuchi, E. Yazaki, K. Kudo, T. Inada, Conserved functions of human Pelota in mRNA quality control of nonstop mRNA. *FEBS Lett* **590**, 3254-3263 (2016).

30. T. Becker, J. P. Armache, A. Jarasch, A. M. Anger, E. Villa, H. Sieber, B. A. Motaal, T. Mielke, O. Berninghausen, R. Beckmann, Structure of the no-go mRNA decay complex Dom34-Hbs1 bound to a stalled 80S ribosome. *Nat Struct Mol Biol* **18**, 715-720 (2011).

31. A. M. van den Elzen, A. Schuller, R. Green, B. Seraphin, Dom34-Hbs1 mediated dissociation of inactive 80S ribosomes promotes restart of translation after stress. *EMBO J* **33**, 265-276 (2014).

32. S. Saito, N. Hosoda, S. Hoshino, The Hbs1-Dom34 protein complex functions in non-stop mRNA decay in mammalian cells. *J Biol Chem* **288**, 17832-17843 (2013).

33. S. Shao, J. Murray, A. Brown, J. Taunton, V. Ramakrishnan, R. S. Hegde, Decoding Mammalian Ribosome-mRNA States by Translational GTPase Complexes. *Cell* **167**, 1229-1240 e1215 (2016).

34. Y. S. Polikanov, T. A. Steitz, C. A. Innis, A proton wire to couple aminoacyl-tRNA accommodation and peptide-bond formation on the ribosome. *Nat Struct Mol Biol* **21**, 787-793 (2014).

Acknowledgments: We thank Fuguo Jiang for his help in model building, Vignesh Kasinath, Junjie Liu, and Basil Greber for discussions about EM data processing and Kelly Nguyen for advice on signal subtraction methods, Meihua Tu and Nathanael Lintner for helpful suggestions, and Fred Ward for comments on the manuscript.

Funding: This work was funded by the Pfizer Emerging Science Fund, and by the NIH (R01-GM065050). **Authors contributions:** Conceptualization: KFM, SL, RD, and JHDC; Investigation and formal analysis: WL, KFM, EM, and JHDC; Writing-original draft: WL and JHDC; Writing-review and editing: all authors. **Competing interests:** KFM, SL, and RD are employed by Pfizer, Inc. The authors have filed patent applications related to this work. **Data and materials availability:** The maps have been deposited with the Electron Microscopy Data Bank under the accession codes EMD-____. Atomic Coordinates and structure factors have been deposited in the Protein Data Bank with accession codes ____.

Fig. 1. Structural analysis of PF846 stalled RNCs. (**A**) Schematic representation of the DNA construct used to prepare PF846 stalled RNCs. (**B**) Stalling of the chimeric PCSK9 nascent chain in *in vitro* translation reactions in the absence (black bar) or presence (white bar) of 100 μM PF846. (**C**) Cryo-EM structure of the stalled CDH1-RNC in the rotated state showing the A/P tRNA (green), P/E tRNA (magenta), CDH1 nascent chain (purple) and PF846 (dark green) with small and large subunit colored cyan and grey, respectively. (**D**) Structure of the stalled CDH1-RNC in the rotated state with A/A tRNA, with A/A and P/E tRNA colored in orange and magenta, respectively.

Fig. 2. Interactions of PF846 with the human ribosome. (**A**-**B**) Phylogenetic analysis of the 28S rRNA binding pocket in eukaryotes (blue) (**A**) and bacteria (red) (**B**). Nucleotides that interact with PF846 are labeled with an asterisk (*). Nucleotides with capital and small letters (AUCG, aucg), are over 98% conserved or 90%-98% conserved, respectively. (**C**-**D**) PF846 chemical and three-dimensional structure,

respectively. (**E**) 28S rRNA residues with direct interactions with the piperidine ring of PF846. Surfaces represent the van der Waals radii of the C, N and O atoms. (**F**-**G**) Interactions of PF846 and nucleotides from 28S rRNA. (**H**) Interaction of the chloro-pyridine ring with U4517, with van der Waals surfaces as in (**E**).

Fig. 3. CDH1 nascent chains and comparisons with other stalled peptides in the ribosome exit tunnel. (**A**) Molecular model of CDH1 nascent chain (magenta) following the 3'-CCA end of A/P tRNA (green) in the ribosome exit tunnel with 28S rRNA (grey), uL22 (orange), uL4 (light green) and PF846 (dark green) highlighted. (**B**-**C**) Superposition of hCMV (blue) and SRP (cyan) nascent chain within the exit tunnel, showing the predicted steric clashes with PF846 (dark green), using with van der Waals surfaces.

Fig. 4. Model of the mechanism of PF846-induced stalling. (**A**) Poor positioning of A/P NC-tRNA 3'-CCA end in the ribosomal P-loop. High-resolution structure of the 3'-CCA end of peptidyl-tRNA (PDB: 1vy4) (*34*) is docked as a rigid body, using nucleotides from 28S rRNA in the PTC as reference. (**B**) C75 modeled as flipped to nearby density without pairing with the P-loop (starting model from PDB: 1vy4) (*34*). (**C**) PF846 binding to the exit tunnel stalls the elongation of the nascent chains in the rotated state, with either A/A NC-tRNA or A/P NC-tRNA. Poor positioning of the 3'-CCA end prevents eEF2-GTP from catalyzing the translocation of hybrid A/P and P/E tRNAs into P/P tRNA and E/E tRNA sites. PF846 can also stabilize the resulting non-rotated ribosome with an empty A site that may signal quality control (QC) pathways.

Supplementary Materials:

Materials and Methods

Figures S1-S11

Tables S1-S2

References (35-52)

Figure 1

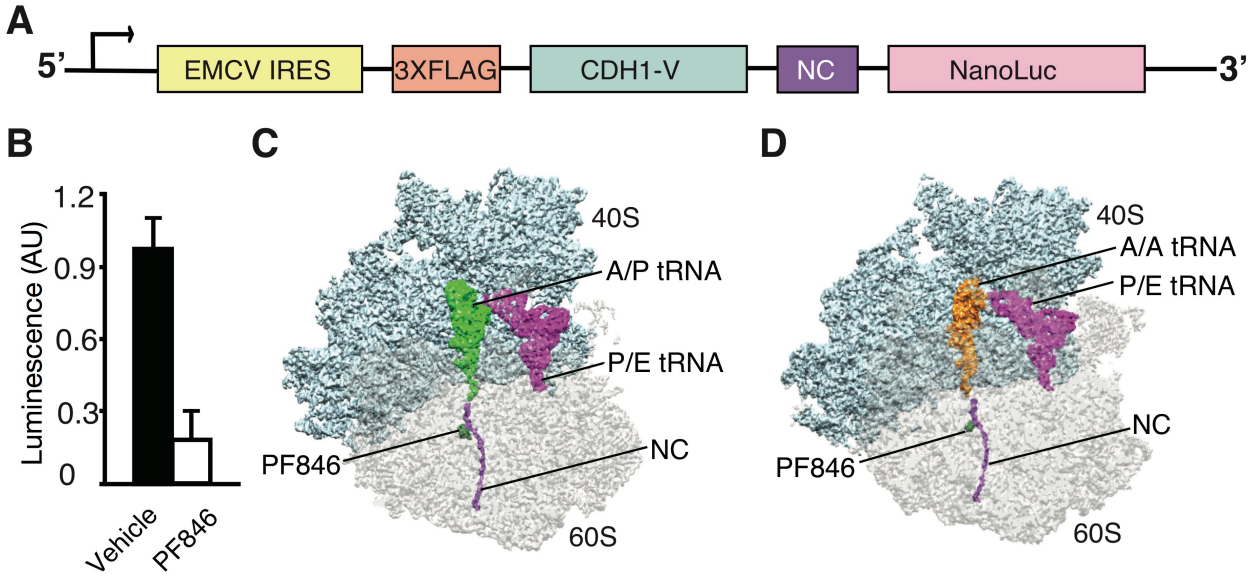
A
5'
EMCV IRES
3XFLAG
CDH1-V
NC
NanoLuc
3'
B
Luminescence (AU)
1.2
0.9
0.6
0.3
0
Vehicle
PF846
C
40S
A/P tRNA
P/E tRNA
PF846
NC
60S
D
40S
A/A tRNA
P/E tRNA
NC
PF846
60S

Figure 2

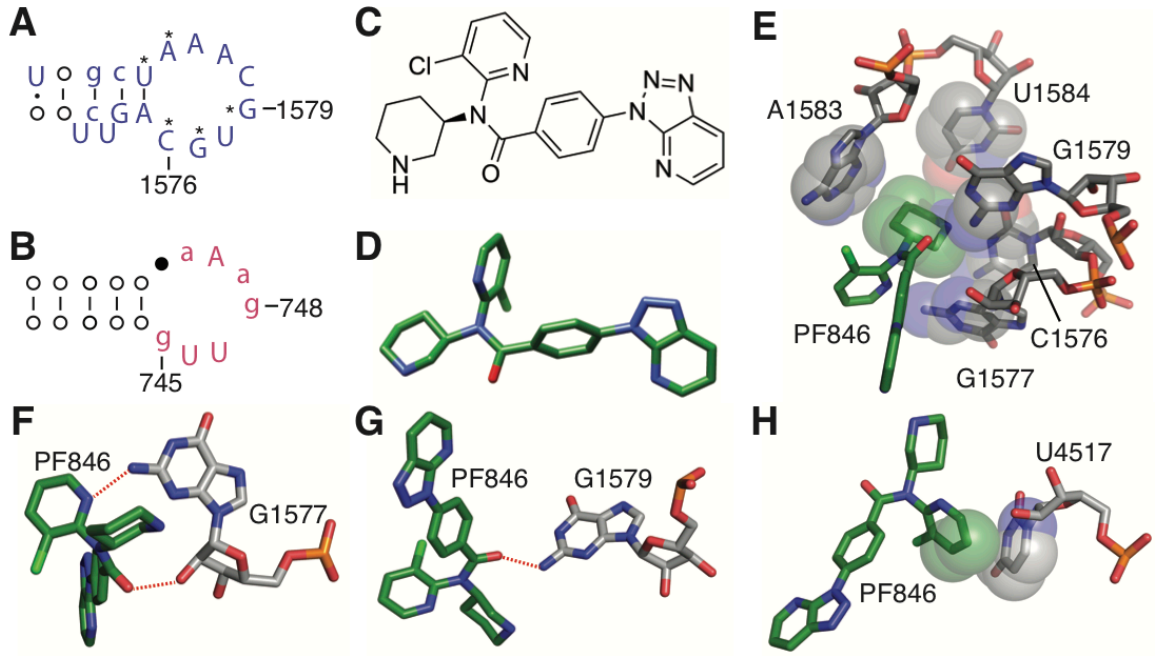
A
1579
1576
B
748
745
C
Cl
N
N=N
N
N
H
O
D
E
A1583
U1584
G1579
PF846
C1576
G1577
F
PF846
G1577
G
PF846
G1579
H
U4517
PF846

Figure 3

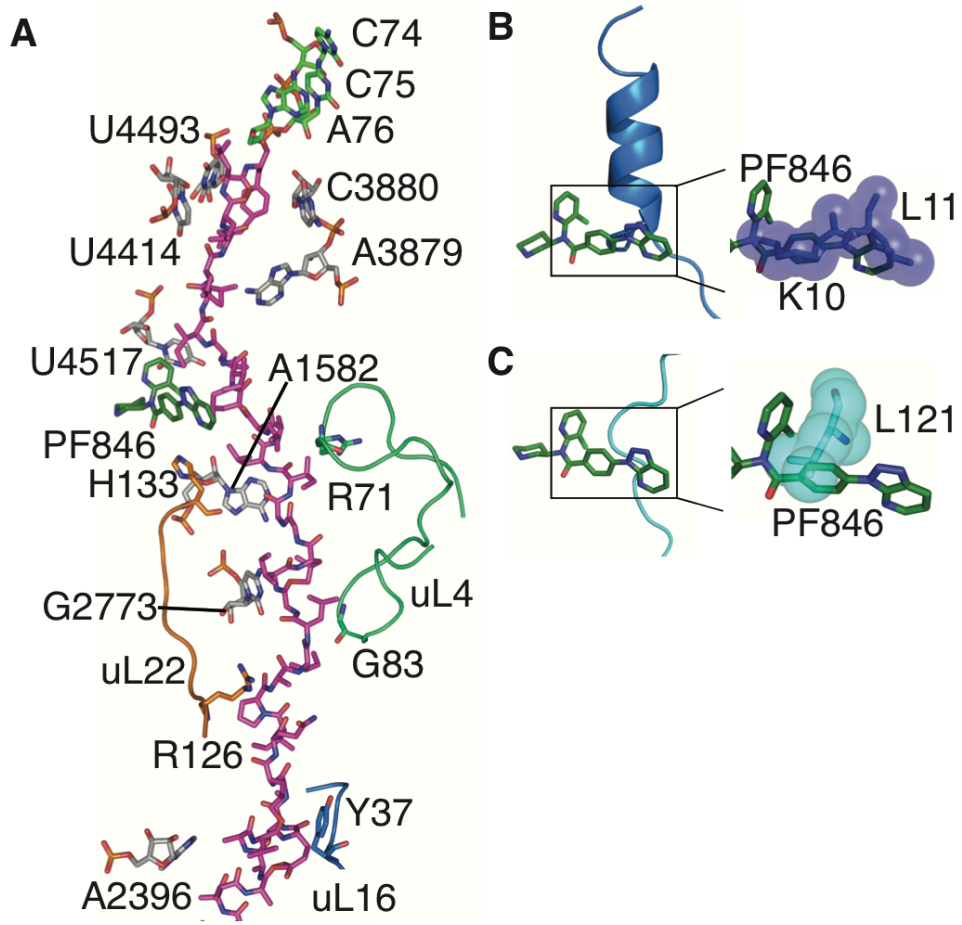
A
C74
C75
U4493
A76
C3880
U4414
A3879
U4517
A1582
PF846
H133
R71
G2773
uL4
uL22
G83
R126
Y37
A2396
uL16
B
PF846
L11
K10
C
L121
PF846

Figure 4

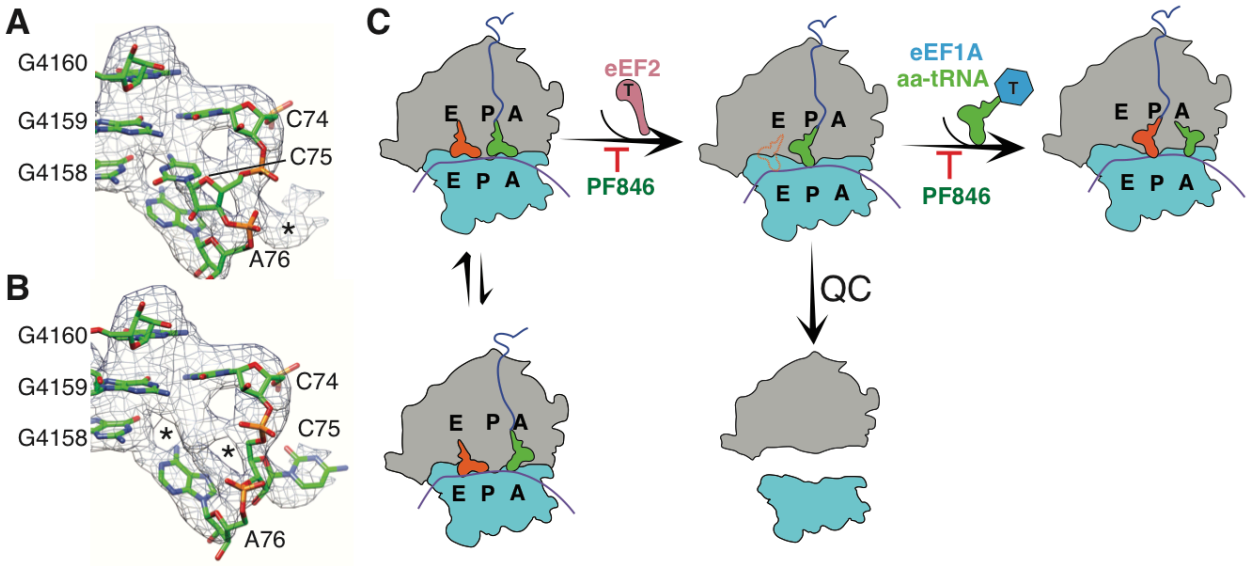
A
G4160
G4159
G4158
C74
C75
A76
B
G4160
G4159
G4158
C74
C75
A76
C
E P A
E P A
eEF2
PF846
eEF1A
aa-tRNA
PF846
QC